

Tunneling, remanence, and frustration in dysprosium-based endohedral single-molecule magnets

Rasmus Westerström,^{1,2,3} Jan Dreiser,² Cinthia Piamonteze,² Matthias Muntwiler,² Stephen Weyeneth,¹ Karl Krämer,⁴ Shi-Xia Liu,⁴ Silvio Decurtins,⁴ Alexey Popov,⁵ Shangfeng Yang,^{5,6} Lothar Dunsch,⁵ and Thomas Greber^{1,*}

¹Physik-Institut, Universität Zürich, Winterthurerstrasse 190, CH-8057 Zürich, Switzerland

²Swiss Light Source, Paul Scherrer Institut, CH-5232 Villigen PSI, Switzerland

³Department of Physics and Astronomy, Uppsala University, Box 516, S-751 20 Uppsala, Sweden

⁴Departement für Chemie und Biochemie, Universität Bern, Freiestrasse 3, CH-3012 Bern, Switzerland

⁵Department of Electrochemistry and Conducting Polymers, Leibniz Institute of Solid State and Materials Research, Dresden, D-01069 Dresden, Germany

⁶Hefei National Laboratory for Physical Sciences at Microscale, Department of Materials Science and Engineering, University of Science and Technology of China, 96 Jinzhai Road, Hefei 230026, China

(Received 18 October 2013; published 27 February 2014)

Paramagnetic atoms inside nanometer sized fullerenes realize robust, and chemically protected, spin systems. Changing the stoichiometry of the endohedral clusters results in a variety of magnetic ground states, as it is demonstrated for $\text{Dy}_n\text{Sc}_{3-n}\text{N}@C_{80}$ ($n = 1, 2, 3$). All three exhibit distinct hysteresis and qualify as single-molecule magnets. In zero field the magnetization of $n = 1$ decays via quantum tunneling, while ferromagnetic coupling of the individual dysprosium moments results in remanence for $\text{Dy}_2\text{ScN}@C_{80}$ and in a frustrated ground state for $n = 3$. The latter ground state turns out to be one of the simplest realizations of a frustrated, ferromagnetically coupled, system.

DOI: [10.1103/PhysRevB.89.060406](https://doi.org/10.1103/PhysRevB.89.060406)

PACS number(s): 75.50.Xx, 33.15.Kr, 71.70.Ej, 75.10.Jm

A single-molecule magnet (SMM) can maintain its magnetization direction over a long period of time [1,2]. It consists of a few atoms that facilitates the understanding and control of the ground state, which is essential in future applications such as high-density information storage or quantum computing [3,4]. The discovery of single-molecule magnets containing one lanthanide ion triggered large interest in $4f$ electron compounds [5,6]. However, the remarkable double decker molecules with one magnetic $4f$ ion have poor remanence: The zero-field magnetization decays rapidly, also via the unavoidable tunneling between states with opposite magnetization. In this respect, dinuclear $4f$ compounds appear to be more robust due to exchange coupling related stabilization of the magnetic moments, [7–11] and there are reports on trinuclear lanthanide ion complexes with [12] and without [13,14] magnetic ground states.

Endohedral fullerenes [15] represent a new family in the class of lanthanide-based single-molecule magnets. They can contain clusters that are not found as free species in nature, and have great potential when it comes to the production of molecular arrays on surfaces. Many of them are particularly stable, survive sublimation, and may be easily imaged [16,17] and manipulated with scanning probes [18,19]. While the $R =$ holmium- or terbium-based $R_3\text{N}@C_{80}$ showed noncollinear paramagnetism [20], it was recently found that the isotropic gadolinium R_3 species shows ferromagnetically coupled collinear paramagnetic behavior [21]. The first endofullerene which displayed hysteresis and qualified as a single-molecule magnet was $\text{DySc}_2\text{N}@C_{80}$. The observed hysteresis is a result of a slow relaxation of the magnetization which is caused by a ligand field that splits the Hund ground state and causes barriers separating states with different magnetization.

However, the symmetry constraints of an isolated Kramers ion with an odd number of electrons, as is Dy^{3+} , did not apply [22].

Here we present results for the complete dysprosium-scandium endofullerene series $\text{Dy}_n\text{Sc}_{3-n}\text{N}@C_{80}$ ($n = 1, 2, 3$) with one, two, or three $4f$ moments inside a nanometer sized closed shell C_{80} cage [see Fig. 1(a)]. This bottom up approach of building a magnet features the unique opportunity to study the effect of adding moments, one by one. The significantly different hysteresis curves demonstrate the decisive influence of the number of magnetic moments and their interactions. In zero field the magnetization of $n = 1$ decays via quantum tunneling, while ferromagnetic coupling of the individual dysprosium moments results in remanence for $n = 2$ and in a frustrated ground state for $n = 3$. Frustration in single-molecule magnets with antiferromagnetic coupling was, e.g., addressed for the case of V_{15} clusters [23], though in the present case noncollinear ferromagnetic coupling leads to frustration.

$\text{Dy}_n\text{Sc}_{3-n}\text{N}@C_{80}$ ($n = 1, 2, 3$) (isomer I_n ; hereafter the isomeric label is omitted for clarity) was produced by a modified Krätschmer-Huffman dc-arc discharge method in a mixture of NH_3 (20 mbar) and He (200 mbar) atmosphere [24–26]. The purity of the chromatographically separated samples with naturally abundant dysprosium was verified by matrix-assisted laser-desorption/ionization time of flight mass spectrometry (MALDI-TOF). For each studied sample, the signals of other components were below the detection limit of about 1% [25,26]. To ensure a low background signal for the superconducting quantum interference device (SQUID) measurements, the molecules were drop cast onto sample holders that were made from kapton foil with a weak linear diamagnetic behavior. This diamagnetic background has been subtracted from the data. For $\text{GdCl}_3 \cdot 6\text{H}_2\text{O}$ (Aldrich) our magnetometer shows at 6 K a Gd magnetic moment of $7.4 \pm 0.2\mu_B$, which compares to $7\mu_B$, as expected from the $\text{Gd}^{3+} \ ^8S_{7/2}$ ground state. To obtain the relaxation times at

*greber@physik.uzh.ch

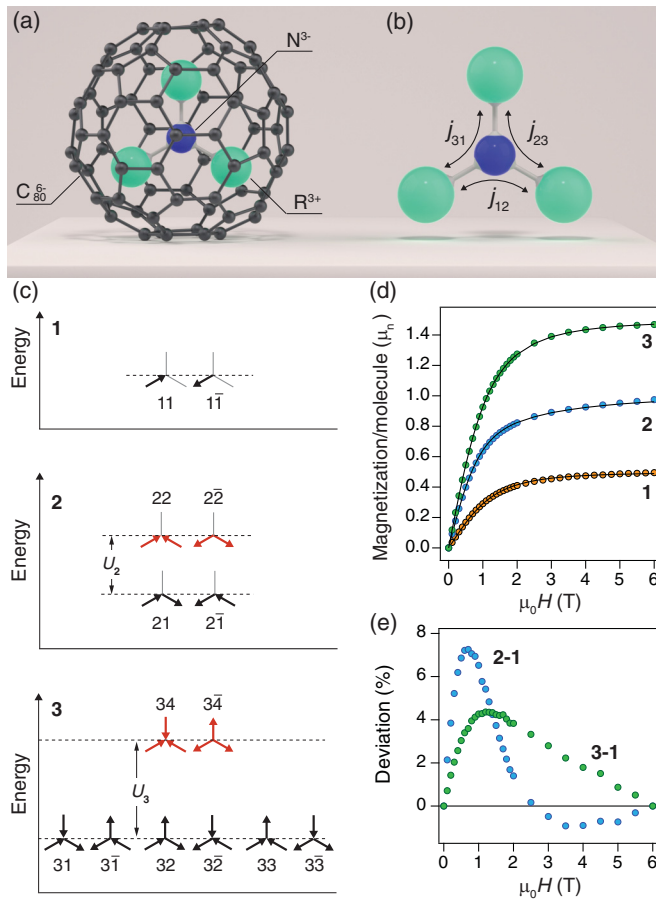


FIG. 1. (Color online) (a) Ball-and-stick model of $R_3N@C_{80}$, R = rare earth (here Dy or Sc). (b) Model of the endohedral $R_3^{3+}N^{3-}$ unit and the corresponding couplings $j_{i,k}$ that are partly mediated across the N^{3-} ion. (c) Ground state magnetic structure for $Dy_nSc_{3-n}N@C_{80}$ based on 2^{n-1} ferromagnetically coupled time reversal symmetric doublets (TRDs) ($n, \pm d$) for $n = 1-3$, where d is the doublet index. The energies U_2 and U_3 are the exchange and dipole barriers for 2 and 3, respectively. (d) Magnetization $m(\mu_0 H)$ of 1–3 at 6 K. The experimental data (dots) are scaled to the magnetic moment per molecule as obtained from the fits of the three ground states in (c). (e) Deviation of m/m_{sat} of 2 and 3 from 1.

elevated temperatures, the ac susceptibility of 2 was measured for varying frequencies of the driving magnetic field.

In zero field the interaction between the magnetic moments may be described with a Hamiltonian reminiscent of Heisenberg and Lines [27,28] of the form

$$\mathcal{H} = \sum_{i \neq k}^n j_{i,k} \mathbf{J}_i \cdot \mathbf{J}_k, \quad (1)$$

where $j_{i,k}$ are the coupling constants and $\mathbf{J}_{i,k}$ the corresponding angular momentum operators on sites i and k , respectively. For Ho and Tb trimetal nitride endofullerenes it was proposed that the magnetic moments $\langle \mathbf{J}_i \rangle$, which are parallel to the expectation values $\langle \mathbf{J}_i \rangle$, remain aligned in the $R^{3+}-N^{3-}$ ligand field [20]. Our findings on 1 [22] and *ab initio* results [29] are in line with the picture where the $\langle \mathbf{J}_i \rangle$ of every Dy^{3+} are uniaxial (anisotropic). This allows the reduction of the ground state problem to a noncollinear Ising model with n

pseudospins [14], which can take two orientations, parallel or antiparallel to the corresponding Dy-N axis. The 2^n solutions for such a Hamiltonian form 2^{n-1} doublets. Each time reversed symmetric doublet (TRD) consists of two time reversed symmetric states with opposite magnetization but with the same energy in zero field [see Fig. 1(c)]. Importantly, the interaction $j_{i,k}$ between different pseudospins lifts the degeneracy of the 2^{n-1} TRDs and gives rise to excitation energies U_n . For 1 the solution is trivial since no interaction occurs. The tunneling rate between the two states in the single doublet determines the magnetization time. For 2 the two TR doublets are split by the interaction $j_{1,2}$. This causes remanence, because demagnetization involves the excitation into the second TRD, or simultaneous tunneling of the two magnetic moments. With the same $j_{i,k}$ between all ions in 3, which is given if the ions sit on an equilateral triangle, we find the four TRDs to split in a group of three magnetic doublets and one nonmagnetic doublet. The fact that 3 shows paramagnetic behavior indicates a negative $j_{i,k}$, i.e., ferromagnetic coupling. This imposes for 3 a sixfold degenerate ground state, where tunneling between these six states enables demagnetization. The appearance of three TR doublets of anisotropic, ferromagnetically coupled pseudospins results in magnetic frustration. Localized ferromagnetism in two dimensions is also found in kagome spin ice [30], while we deal here with a finite system of three pseudospins. Notably, this is analogous to the case of isotropic spins on an equilateral triangle, where frustration is caused by an antiferromagnetic exchange interaction [31].

The pseudospin structures of the ground states for 1–3 are shown in Fig. 1(c). The level scheme of the 2^{n-1} TR doublets is reflected in the magnetization curves. The magnetic moment of a given molecule corresponds to the vectorial sum of the n individual moments. In a magnetic field the TRDs undergo Zeeman splitting, and since they are different for 1–3, distinct susceptibility beyond scaling with n is observed. In Fig. 1(d) the magnetizations at a temperature of 6 K are displayed as a function of the applied field. The curves for the three molecules are different, which is not only due to the number of Dy atoms per molecule, as can be seen in Fig. 1(e). The relative differences between the three molecules amount up to 10%, which allows the extraction of the different ground state parameters.

The magnetization curves are reminiscent of Brillouin functions, though, in the present case, the Dy^{3+} moments do not align along the magnetic field and the degeneracy of the ${}^6H_{15/2}$ ground state is partly lifted by the ligand field. Assuming randomly frozen, independent molecules reduces the saturation magnetization to half the value of the maximum magnetization of free molecules, since only the projection on the field direction contributes. Together with the given structure of the TRDs, we can extract the magnetic moments μ_n and the TRD splittings U_2 and U_3 [Fig. 1(c)] from a comparison of simulated magnetization curves with the experiment. The solid lines in Fig. 1(d) represent the best fits of these simulations to the measured data.

The magnetic moment of 1 of $\mu_1 = 9.37 \pm 0.06 \mu_B$ agrees with a large m_J ground state along the Dy-N axis. For 2, $\mu_2 = 8.75 \pm 0.13 \mu_B$, and the splitting U_2 between the two TRDs gets 0.96 ± 0.1 meV. For 3, $\mu_3 = 9.46 \pm 0.05 \mu_B$, and

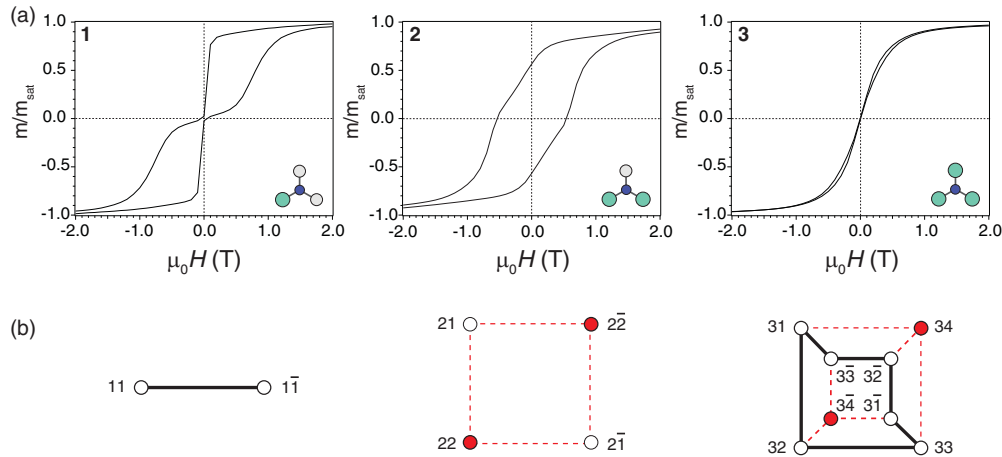


FIG. 2. (Color online) (a) Hysteresis curves for 1–3 recorded using SQUID magnetometry at 2 K with a field sweep rate of 0.8 mT s^{-1} . The data of 1 are reproduced from Ref. [22]. (b) Hilbert space topology of the 2^n pseudospin states ($n, \pm d$) in 1–3. Solid lines correspond to single-tunneling events of one magnetic moment between two states at the same energy. Red dashed lines involve an energy barrier, which is due to exchange and dipolar coupling.

a value of U_3 of $0.3 \pm 0.2 \text{ meV}$, a weaker coupling than in 2.

Figure 2(a) displays magnetization curves at 2 K taken with a field sweep rate of 0.8 mT s^{-1} for 1–3. The observed hystereses demonstrate that the rate at which the magnetization relaxes to its equilibrium is slow compared to the measurement time. The distinct shapes indicate how strongly the number of moments and their interactions influences the response to external magnetic field changes. For applications the remanence, i.e., the memory of magnetization history in zero field, is of particular interest. There is large “remanence” for 2, as compared to a sharp drop of the magnetization at low fields for 1, and a narrow hysteresis with vanishing zero-field magnetization for 3. It is a clear consequence of the magnetic interaction between the endohedral dysprosium ions in 2 and 3, which is partially mediated by the central N^{3-} ion. For 1 the enhanced tunneling of magnetization in the absence of an applied field is seen in the abrupt jump of the magnetization when approaching the $\mu_0 H = 0$ point. The narrow hysteresis of 3 makes it the softest single-molecule magnet of the three. This is due to magnetic frustration of the ground state, which suppresses remanence. The Zeeman splitting between the lowest and the first excited state in 3 is smaller than in 1, which allows more efficient flipping of the magnetization, also in an applied field. So far frustration was not realized in trinuclear magnetic molecules as the relevant mechanism for zero-field demagnetization [13,14,20]. In contrast to 1 and 3, the reversal of magnetization in 2 requires a *simultaneous* flip of both magnetic moments or the crossing of the barrier U_2 , which consequently stabilizes the zero-field magnetization. The barrier has contributions from the exchange energy and the dipolar coupling of the two moments $\vec{\mu}_2$.

In Fig. 2(b) the Hilbert space of the time reversal doublets ($n, \pm d$) for the three molecules [see Fig. 1(c)] are shown. $\pm d$ are the indices of the two states in the given TRDs. The 2^n states are connected by a network of single-tunneling transitions that correspond to the flipping of one magnetic moment. For 1 and 3 all ground state TRDs are connected by single-tunneling

transitions at the ground state energy, which is an intrinsic demagnetization mechanism that suppresses remanence. For 2 there is no single-tunneling path connecting the ground state TRD, and a single-tunneling event costs the energy U_2 .

The U_2 barrier is also reflected in the temperature dependence of the zero-field magnetization decay times. Below 5 K a double exponential was fitted to the decay data [Fig. 3(a)], as was done for the case of $\text{DySc}_2\text{N@C}_{80}$, where this behavior was ascribed to different hyperfine interactions of different Dy isotopes [22]. The resulting decay times for the slower process τ_A are displayed on a logarithmic scale versus the reciprocal temperature in Fig. 3(b). A 100 s blocking temperature of about 5.5 K is determined, which is among the highest temperatures reported for single-molecule magnets [8,9]. Higher temperatures were accessed using ac magnetic susceptibility measurements and the corresponding relaxation times are displayed as open symbols in Fig. 3(b). Clearly, the relaxation times show two temperature regimes, indicating distinct relaxation mechanisms. Down to 2 K

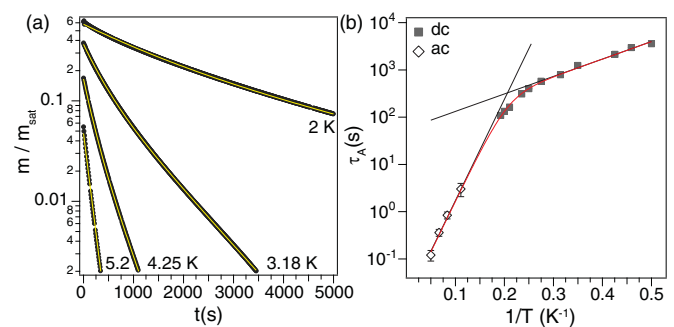


FIG. 3. (Color online) (a) Zero-field relaxation curves for 2 after saturation at $\mu_0 H = 7 \text{ T}$. m_{sat} is the magnetization at 7 T. The line corresponds to a fit of a double ($T < 4.5 \text{ K}$) and a single ($T > 4.5 \text{ K}$) exponential. (b) Corresponding relaxation times τ_A as a function of inverse temperature. Open symbols are ac susceptibility results. The red line is the best fit of Eq. (2).

the zero-field relaxation times do not show a temperature independent region, as observed for a single pseudospin flip tunneling regime in 1 [22], because this relaxation mechanism is suppressed in the ground state of 2 by the barrier U_2 .

Fitting the lifetimes τ_A to

$$\tau_A = \frac{\tau_1 \tau_2}{\tau_1 + \tau_2} \quad (2)$$

leads with $\tau_\ell = \tau_{2,\ell}^0 \exp(U_{2,\ell}^{\text{eff}}/k_B T)$ to the solid curve in Fig. 3(b). The effective energy barriers for magnetization reversal get $U_{2,1}^{\text{eff}} = 0.73 \pm 0.04$ meV and $U_{2,2}^{\text{eff}} = 4.3 \pm 0.1$ meV with preexponential factors $\tau_{2,1}^0 = 56.5 \pm 9.8$ s and $\tau_{2,2}^0 = 12.0 \pm 1.3$ ms, respectively. The lower barrier $U_{2,1}^{\text{eff}}$ corresponds to the energy gap between the two TR doublets [Fig. 1(c)]. The higher barrier $U_{2,2}^{\text{eff}}$ is similar to the one found in a Co_2Dy_2 compound [10], and must be related to relaxation via higher lying excited states. It is, however, much smaller than the theoretical result in Refs. [29] and [10], respectively. As in 1 [22], the prefactors $\tau_{2,\ell}^0$ in 2 are, compared to other Dy-based single-molecule magnets [5,10], remarkably large. This is taken as an indication that the phase spaces for tunneling and excitations leading to a decay of the magnetization are

particularly small, which must be due to the peculiar protection of the magnetic moments in the closed shell C_{80} cage.

In summary, the three dysprosium-based endofullerenes $\text{Dy}_n\text{Sc}_{3-n}\text{N}@C_{80}$ ($n = 1, 2, 3$) are identified as single-molecule magnets with three different ground states. The present pseudospin model for the ground states is expected to be generally valid for uniaxially anisotropic $R_3\text{N}@C_{80}$ endofullerenes. The distinct hysteresis curves reflect on how dramatic changes can be caused by stoichiometry and interaction in single-molecule magnets. The observed large remanence in 2 is due to an energy barrier for flips of individual $4f$ moments. For the trinuclear nitrogen-cluster $\text{Dy}_3\text{N}@C_{80}$ the ferromagnetic coupling results in a frustrated ground state that suppresses remanence regardless of the exchange and dipolar barrier. These findings demonstrate the crucial role of magnetic frustration for the suppression of magnetization blocking in single-molecule magnets.

The project is supported by the Swiss National Science Foundation (SNF projects 200021 129861 and 147143), the Swedish Research Council (350-2012-295), and the Deutsche Forschungsgemeinschaft (DFG Project No. PO 1602/1-1). We acknowledge discussions with one of the authors of Ref. [29].

- [1] R. Sessoli, D. Gatteschi, A. Caneschi, and M. A. Novak, *Nature (London)* **365**, 141 (1993).
- [2] D. Gatteschi and R. Sessoli, *Molecular Nanomagnets* (Oxford University Press, New York, 2006).
- [3] M. N. Leuenberger and D. Loss, *Nature (London)* **410**, 789 (2001).
- [4] L. Bogani and W. Wernsdorfer, *Nat. Mater.* **7**, 179 (2008).
- [5] N. Ishikawa, M. Sugita, T. Ishikawa, S.-y. Koshihara, and Y. Kaizu, *J. Am. Chem. Soc.* **125**, 8694 (2003).
- [6] D. N. Woodruff, R. E. P. Winpenny, and R. A. Layfield, *Chem. Rev.* **113**, 5110 (2013).
- [7] Y.-N. Guo, G.-F. Xu, W. Wernsdorfer, L. Ungur, Y. Guo, J. Tang, H.-J. Zhang, L. F. Chibotaru, and A. K. Powell, *J. Am. Chem. Soc.* **133**, 11948 (2011).
- [8] J. D. Rinehart, M. Fang, W. J. Evans, and J. R. Long, *J. Am. Chem. Soc.* **133**, 14236 (2011).
- [9] J. D. Rinehart, M. Fang, W. J. Evans, and J. R. Long, *Nat. Chem.* **3**, 538 (2011).
- [10] K. C. Mondal, A. Sundt, Y. Lan, G. E. Kostakis, O. Waldmann, L. Ungur, L. F. Chibotaru, C. E. Anson, and A. K. Powell, *Angew. Chem. Int. Ed.* **51**, 7550 (2012).
- [11] F. Habib and M. Murugesu, *Chem. Soc. Rev.* **42**, 3278 (2013).
- [12] J. Tang, I. Hewitt, N. T. Madhu, G. Chastanet, W. Wernsdorfer, C. E. Anson, C. Benelli, R. Sessoli, and A. K. Powell, *Angew. Chem. Int. Ed.* **45**, 1729 (2006).
- [13] J. Luzon, K. Bernot, I. J. Hewitt, C. E. Anson, A. K. Powell, and R. Sessoli, *Phys. Rev. Lett.* **100**, 247205 (2008).
- [14] L. F. Chibotaru, L. Ungur, and A. Soncini, *Angew. Chem.* **120**, 4194 (2008).
- [15] A. Popov, S. Yang, and L. Dunsch, *Chem. Rev.* **113**, 5989 (2013).
- [16] M. Treier, P. Ruffieux, R. Fasel, F. Nolting, S. Yang, L. Dunsch, and T. Greber, *Phys. Rev. B* **80**, 081403 (2009).
- [17] S. Zhang, J. Zhang, J. Dong, B. Yuan, X. Qiu, S. Yang, J. Hao, H. Zhang, H. Yuan, G. Xing, Y. Zhao, and B. Sun, *J. Phys. Chem. C* **115**, 6265 (2011).
- [18] M. J. Butcher, J. W. Nolan, M. R. C. Hunt, P. H. Beton, L. Dunsch, P. Kuran, P. Georgi, and T. J. S. Dennis, *Phys. Rev. B* **67**, 125413 (2003).
- [19] T. Huang, J. Zhao, M. Feng, A. Popov, S. Yang, L. Dunsch, and H. Petek, *Chem. Phys. Lett.* **552**, 1 (2012).
- [20] M. Wolf, K.-H. Müllera, D. Eckerta, Y. Skourskib, P. Georgia, R. Marczaka, M. Krausea, and L. Dunsch, *J. Magn. Magn. Mater.* **290**, 290 (2005).
- [21] B. Náfrádi, Á. Antal, Á. Pásztor, L. Forró, L. F. Kiss, T. Feher, E. Kováts, S. Pekker, and A. Jánossy, *J. Phys. Chem. Lett.* **3**, 3291 (2012).
- [22] R. Westerström, J. Dreiser, C. Piamonteze, M. Muntwiler, S. Weyeneth, H. Brune, S. Rusponi, F. Nolting, A. Popov, S. Yang, L. Dunsch, and T. Greber, *J. Am. Chem. Soc.* **134**, 9840 (2012).
- [23] G. Chaboussant, S. T. Ochsenbein, A. Sieber, H.-U. Güdel, H. Mutka, A. Müller, and B. Barbara, *Europhys. Lett.* **66**, 423 (2004).
- [24] L. Dunsch, M. Krause, J. Noack, and P. Georgi, *J. Phys. Chem. Solids* **65**, 309 (2004).
- [25] S. Yang, A. A. Popov, and L. Dunsch, *J. Phys. Chem. B* **111**, 13659 (2007).
- [26] S. Yang, A. A. Popov, C. Chen, and L. Dunsch, *J. Phys. Chem. C* **113**, 7616 (2009).
- [27] M. E. Lines, *J. Chem. Phys.* **55**, 2977 (1971).
- [28] J. Luzon and R. Sessoli, *Dalton Trans.* **41**, 13556 (2012).
- [29] V. Vieru, L. Ungur, and L. F. Chibotaru, *J. Phys. Chem. Lett.* **4**, 3565 (2013).
- [30] A. S. Wills, R. Ballou, and C. Lacroix, *Phys. Rev. B* **66**, 144407 (2002).
- [31] M. Seo, H. K. Choi, S. Y. Lee, N. Kim, Y. Chung, H. S. Sim, V. Umansky, and D. Mahalu, *Phys. Rev. Lett.* **110**, 046803 (2013).